Surface roughness analysis of medical grade titanium sheets formed by single point incremental forming

Shakir Gatea[a] and Hengan Ou[b]

[a] Department of Materials Engineering, Faculty of Engineering, University of Kufa, Al-Najaf, Iraq

[b] Department of Mechanical, Materials and Manufacturing Engineering, Faculty of Engineering, University of Nottingham, Nottingham, NG7 2RD, UK

Abstract

Single point incremental forming (SPIF) process has proven benefits in terms of formability, flexibility, and low cost as compared to conventional sheet forming, although it has some issues such as dimensional accuracy and low quality of surface finish for some materials. The SPIF is considered as a potential method of producing customised medical parts such as craniofacial implants using a titanium sheet. This investigation aims to analyse the overall surface roughness of grade 1 pure titanium along the wall of the hyperbolic truncated cone formed by the SPIF process with different forming parameters (i.e., forming tool diameter, step size, and feed rate). Focus variation microscopy was used to measure the surface roughness experimentally along the wall of the truncated cone. Abaqus/Explicit was used to predict the equivalent stress and equivalent plastic strain along the wall of the truncated cone part from the top to the fractured region to evaluate the relationship between the stress, strain, and roughness distribution. It was found that the surface roughness changes with the deformed part height and rough surface could be produced in the region of high equivalent stress and low equivalent plastic strain. Such a surface roughness and equivalent stress and plastic strain correlation has a clear implication to the design and the surface quality of sheet parts made by SPIF.

Keywords: SPIF, Surface roughness, Grade 1 pure titanium, Forming parameters

Corresponding authors: Shakir Gatea, Shakir.Gatea@uokufa.edu.iq *and* Hengan Ou, H.Ou@nottingham.ac.uk

1. Introduction

In the single point incremental forming (SPIF) process, the blank sheet is converted to the appropriate shape by applying load in incremental mode using a hemispheric tool that follows certain tool path operated by using a computer numerical control (CNC) machine. The SPIF process is an attractive concept for small scale and customised production. The accurate evaluation and analysis of the surface roughness of the SPIF components is considered to be one of the key challenges in order to move the SPIF process to the next stage of technical maturity.

Several articles on the surface roughness of the SPIF components have been published, all of which aim at achieving reduced surface roughness of the deformed parts through the SPIF process. Several parameters, e.g. step size, feed rate, tool rotation speed and direction, tool material, tool path, and wall angle, have been taken into account to select a suitable values of parameters to enhance the surface quality [1]. The SPIF part's surface roughness was measured in two directions, in the advancing direction of the tool and the perpendicular one. The roughness in the advancing direction of the tool was observed to be roughly the half the roughness in the perpendicular direction [2]. The tool path of the two-point incremental sheet forming was evaluated and optimized to achieve the best surface quality. It was found that the correct choice of the scallop height and step size was effective to help improve the surface quality of the final parts [3]. Experimentally, the effect of the SPIF tool rotation on the surface quality of AA7075-T0 sheets has been emphasised. It was pointed out that the surface roughness decreased from a non-rotating tool by less than 10 percent as compared to the same process using a rotating tool [4]. The effect of high tool rotational speeds and feed rate on the surface roughness of Al3003-H14 sheets was investigated and analysed in the SPIF process. The findings showed that the surface roughness is more sensitive to the step size and the ratio of forming wall angle to tool diameter [5]. The influence of the forming parameters on the surface of medical implants produced through the SPIF process was investigated based on experimental testing. The results showed that the friction condition between the forming tool and the blank surface and the roughness of the forming tool affected the surface quality of the medical parts although the diameter of the tool had a less effect on the roughness of the surface of the deformed part [6]. The effect of tool diameter, the forming angle, and the step size of the SPIF process on the surface roughness of Al5052 sheets was investigated based on Box-Behnken method. It was found that the roughness of the deformed parts decreased with the increase of tool diameter and forming angle. On the other hand, the increase in step size resulted in an increased roughness

until the reach of a certain forming angle [7]. To assess the effect of hot SPIF parameters on surface quality, the surface roughness of three lightweight alloy sheets (magnesium AZ31B-O, aluminium AA2024-T3, and titanium Ti6Al4V) was measured by using a hot SPIF process with various parameters. The surface roughness increases were found with an increased draw angle and energy input [8]. An algorithm based on the specific critical edges was used to generate the tool path of the SPIF process. There was an evidence that the critical edges of the deformed components had a better surface finish, particularly in the non-horizontal edge [9]. A SPIF tool was constructed from acetal to investigate the effect of forming tool material on the surface quality of the aluminium sheet. The use of acetal tools in comparison to traditional SPIF tool made of carbide steel shows that isotropic surface roughness may be produced. [10].

A mathematical relationship between the forming parameters and surface roughness was derived using response surface methodology to optimise the surface roughness of AA050 aluminium alloy sheets deformed by the SPIF process. The results showed that the suitable selection of SPIF parameters could be employed to enhance the surface roughness of deformed parts [11]. An oblique roller SPIF tool was developed to reduce the effect of the friction on the surface finish of AA6111, AA2024, AA1100, and AA5052 sheets. It was found that the friction can be reduced, and good surface quality parts could be produced when replacing the traditional SPIF tool with a roller-based tool [12]. Different techniques (Genetic Programming, Artificial Neural Networks, and Support Vector Regression) have been used to build predictive models for the surface roughness of extra deep drawing steel parts through SPIF process. The step size, tool diameter, feed rate, lubricant, and forming angle were considered as variables in these models. The predicted surface roughness values showed that such models could be used with a small percentage of the error to potentially predict surface roughness [13]. Nakajima test was used to construct the forming limit diagram of medical-grade titanium sheets at necking and fracture. The forming limit curve at fracture was compared with the fracture date of the SPIF process. The results showed the capability of the Nakajima test to describe the fracture of medical-grade titanium sheets of SPIF [14]. Using an artificial neural network, the average surface roughness of the AA5052-H32 SPIF components was evaluated. The predicted surface ruggedness values were compared with experimental results. The neural network was found to be capable of predicting the surface roughness of SPIF formed components with reasonable precision [15]. The finite element approach was used to investigate the effect of ultrasonic vibration on the incremental sheet forming process of bi-metal

steel/titanium sheets. Ultrasonic vibration has been shown to increase the surface quality by reducing the friction coefficient between the forming tool and the bi-metal steel/titanium sheet [16]. A multistage SPIF process with different tool shapes (flat and hemispherical tools) was employed to develop a flat-base aerospace component. The results showed that complex geometers could be produced by multistage SPIF and flat forming tool was considered suitable for flat-base components [17]. Various tool paths have been generated based on a computer-aided manufacturing approach to improving the quality of SPIF components. It was found that this approach could improve the surface quality of the produced parts [18]. The effects of workpiece geometry, tools size and sheet thickness on the formability of polycarbonate sheets have been studied by means of experimental work and a finite element simulation. The findings have shown that the geometry of the workpiece and the tool size have an important influence on formability, while the thickness of the sheet has a minor effect [19].

To obtain the best correlation between the SPIF parameters and their effect on DC01, AA1050, and Cu-Be2 sheets surface roughness, the response surface methodology was combined with Taguchi's grey relational analysis. The variance analysis showed that the lubricant and the type of material had a major effect on the surface roughness of the deformed parts [20]. A parametric study was conducted to evaluate the effect of resistance SPIF parameters on the surface finish of Ti6Al4V titanium alloy sheets using the Taguchi method and analysis of variance. It was concluded that the step size, lubricant, and feed rate have a significant effect on the surface roughness of the deformed parts and the best surface finish could be produced when a graphite-based anti-seize compound was utilized as a lubricant [21]. A multi-point tool was used to improve the surface finish of grade 202 austenitic stainless-steel parts produced by the SPIF process and the roughness results were compared with the conventional SPIF tool using a three-dimensional surface roughness test. The results of the study revealed that the multi-point tool works in order to improve SPIF parts' surface finish compared to conventional tools [22]. Elastic deflection and plastic deformation were considered to establish an analytical surface roughness model to predict the surface quality of the ISF components. The results showed there is a relationship between the surface scallop and thickness of the deformed part [23]. A predictive toolpath control algorithm was proposed to reduce the geometric errors of complex SPIF components. The results showed that the closed-loop path minimized geometric errors [24]. The finite element simulation method has been developed to

simulate localised convective heating in the SPIF process. It was found that the method developed could be used as part of the temperature-dependent finite element model of the SPIF process [25].

It is evident from literature that efforts have been made to determine the effect of SPIF parameters on the surface quality of the deformed components in a specified area (not the entire surface along the wall of the product) based on the experimental investigation or using empirical and analytical models. From the above investigations, it can be concluded that there is a knowledge gap about the impact of the SPIF parameters (i.e., tool size, step size, and feed rate) on the surface roughness of the deformed parts; some studies indicate that the increase in the values of forming parameters improves the surface quality, while others argue that the increase in the values of forming parameters has a detrimental influence on the surface quality. Furthermore, there is a lack of specific knowledge regarding the distribution of the overall surface roughness along the height of the deformed parts and the relationship between surface quality and stress and strain distribution. In combination of the experimental work and finite element analysis, this investigation aims to provide an in-depth understanding of the influence of SPIF parameters on the overall surface roughness of grade 1 pure titanium sheets along the wall of the hyperbolic truncated cone and to establish a relationship between the distribution of the equivalent stress, equivalent plastic strain, and the surface roughness.

2. Experimental setup and FE modelling

This research was performed using a grade 1 pure titanium sheet of 0.7 mm thickness. Tensile samples were designed and manufactured according to the BS EN10002-1 British specification for evaluating the mechanical characterisation of the titanium sheet and tested at room temperature. The mechanical properties of grade 1 pure titanium are given in Table 1. To carry out the experimental work of the SPIF tests, a clamping frame was designed and manufactured to hold the sheet of the pure titanium with size 140 mm x 140 mm during the forming process. This frame is mounted on the table of a HURCO (VM10) CNC milling machine as shown in Figure 1. A tool path was generated to form the hyperbolic truncated cone with varying wall angles under different conditions of SPIF parameters. To gain a better understanding of the surface roughness distribution of the titanium sheets along the deformed hyperbolic truncated cone wall under various SPIF parameters, the SPIF test was performed with different values of the tool diameter (8, 10, and 15 mm), step size (0.2, 0.4, and 0.6 mm), and feed rate (1000, 2000, and 3000 mm/min). Rocol RDT

grease compound was used as a lubricant between the Ti sheet and the forming tool to reduce the friction effect and improve the surface finish.

Table 1 Mechanical properties of medical grade 1 pure titanium.

Young's modulus	Poisson's ratio	Yield stress	Ultimate tensile stress	Density
108 GPa	0.34	223.49 MPa	363 MPa	4505kg/m^3

Figure 1 Experimental setup of single point incremental forming process on CNC milling machine and deformed specimens.

The surface roughness of the formed components is considered an important parameter in the SPIF process for evaluating the quality of the product as well as having a major impact on the product's aesthetic appearance and functionality. The average roughness parameter (R_a) is commonly used to quantify the surface roughness of the products. In the present investigation, the focus variation microscopy (Alicona G4 Infinite Focus (IF) system) was used to measure surface roughness of as-received sheet and along the deformed hyperbolic truncated cone wall of the pure Ti sheet as shown in Figure 2. The use of the infinite Focus system is according to the non-contact optical 3D measurement procedure. The Infinite Focus system is a metrological tool used to measure surface roughness by focusing variation. Throughout this study, the wall of the hyperbolic truncated cone was scanned by the infinite Focus system from the transition zone between the top of the truncated cone and inclined wall to the transition zone between the inclined wall of the truncated cone and the bottom surface as shown in Figure 2. Each measurement of roughness was repeated three times and the average of the readings was taken to improve the precision of the measurement.

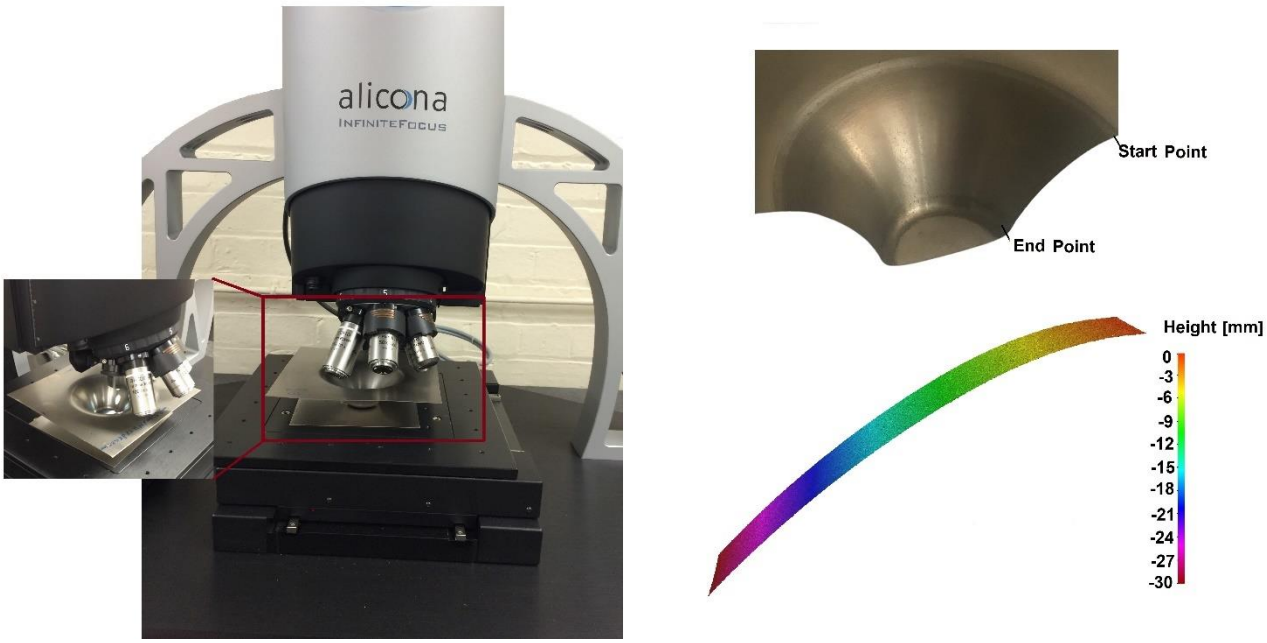

Figure 2 Experimental setup of surface roughness test using Alicona G4 Infinite Focus (IF) system.

To evaluate and analyse the equivalent stress and equivalent plastic strain along the wall of SPIF parts, a 3D elasto-plastic finite element model was established using Abaqus/Explicit. Hyperbolic

truncated cone shape with varying wall angles (from 22° to 80°) was utilised as a benchmark in this investigation. Figure 3 shows the geometric shape of the hyperbolic truncated cone profile and the finite element model of the SPIF process. The forming tool, blank-holder, and backing-plate were all modelled as analytical rigid bodies. 8-node hexahedral solid elements with reduced integration (C3D8R) were employed to mesh the pure titanium sheet. To consider the effect of friction between the pure titanium sheet and the forming tool and between the titanium sheet and fixtures (blank holder and backing plate), Coulomb's friction model with a coefficient of 0.1 was applied.

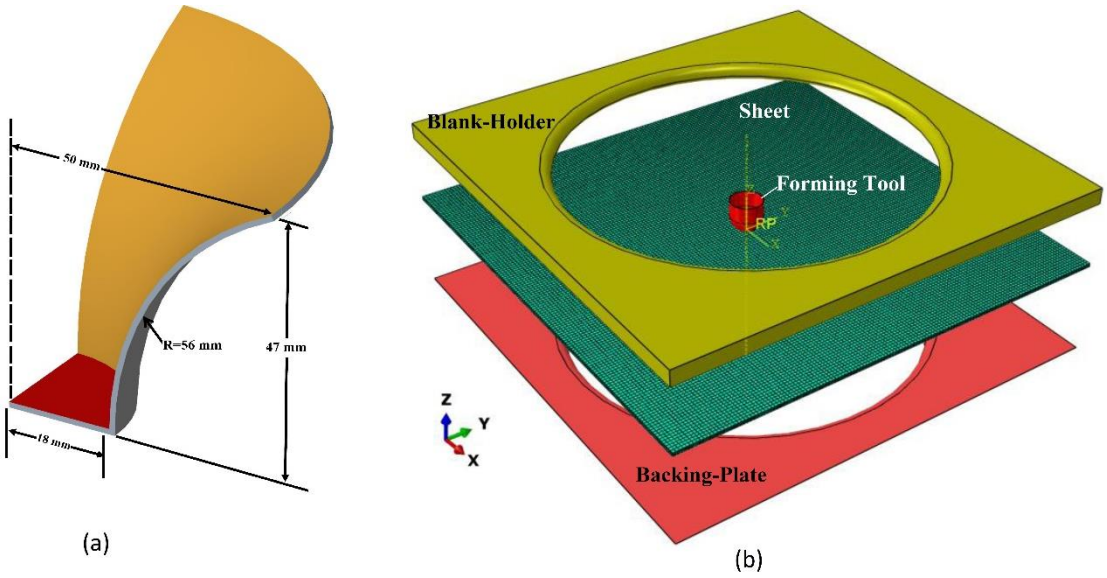

Figure 3: (a) Geometric shape of hyperbolic truncated cone part and (b) finite element model of single point incremental forming.

3. Results and discussion

The surface roughness of the as-received sheet was measured using the Alicona G4 Infinite Focus (IF) system along the path equal to the fracture depth of the deformed part (32 mm). This measurement data was used as a reference in order to determine and analyse the effect of the SPIF parameters, i.e., tool size, step size, and feed rate on the surface quality of the grade 1 pure titanium deformed part. The surface profile of the as-received Ti sheet is shown in Figure 4 with an average roughness Ra value equal to 0.1295 µm. From the figure, it is clear that the roughness profile is uniform along the measured path, and there is no clear change in the height of the maximum wave.

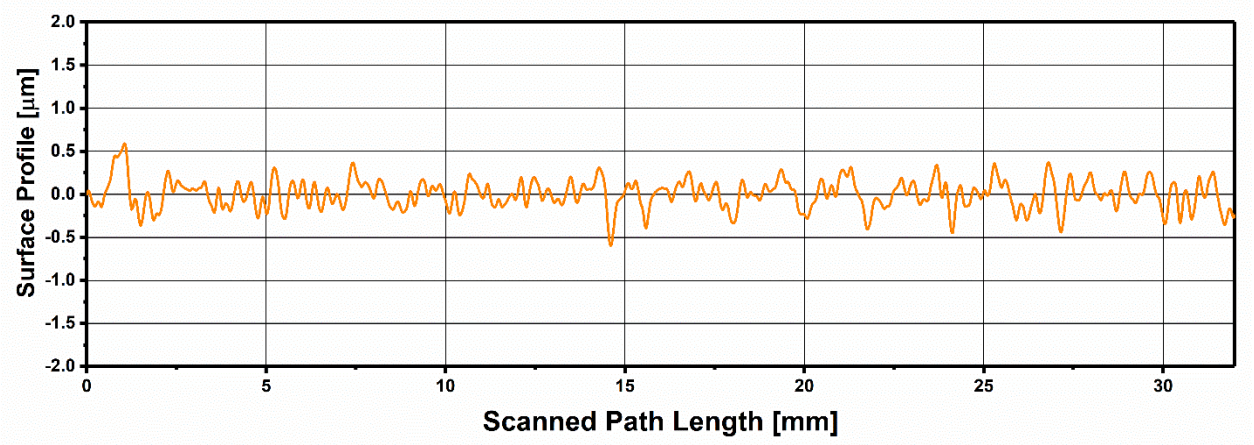

Figure 4 The surface roughness profile of undeformed pure titanium sheet.

Under various SPIF processing conditions, the roughness was measured in the direction of incremental depth on the inner surface of the hyperbolic truncated cone. Figure 5 shows the effect of the tool diameter, step size, and feed rate on the average surface roughness of the produced components. It is evident from the figure that the Ra decreases with increased tool size and step size, the same trend has been identified in the previous studies [3, 26], while the average value of the roughness is decreased then increased when the feed rate was changed from 1000 mm/min to 3000 mm/min, these results are consistent with previous study of Silva et al. [27]. The Ra is decreased by 21% and 16.5% when the step size increased from 0.2 mm to 0.6 mm, and the tool diameter is changed from 10 mm to 15 mm, respectively. The effect of feed rate on the surface roughness is inconsistent. There was 14.5% surface roughness reduction when the feed rate was increased from 1000 mm/min to 2000 mm/min and 10.9% when the feed rate is 3000 mm/min. The decrease in surface roughness with an increase in tool size can be attributed to an increase in the overlap between the nearby paths.

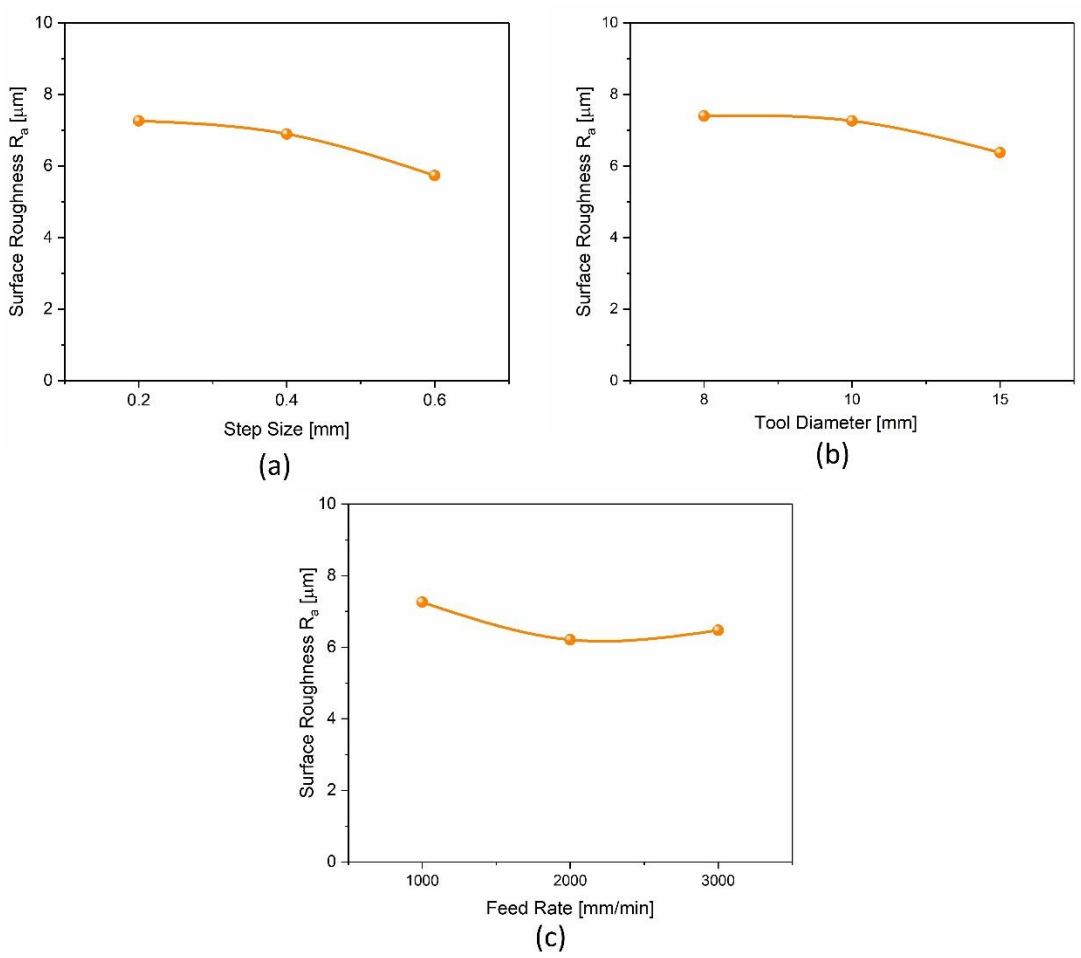

Figure 5 Effect of SPIF process parameters on the average surface roughness: (a) effect of step size, (b) effect tool diameter, and (c) effect of feed rate.

The surface roughness distribution along the wall of the truncated cone was measured from the top to the bottom of the cone under different conditions as shown in Figure 6. Figure 7 demonstrates the distribution of surface profiles under different SPIF conditions. It is noted that when the SPIF parameters are altered, the waviness height and the spacing between the waviness could be changed. From the figure shown the waviness height is reduced when the step size and tool diameter are increased, and better surface finish is produced. The distribution of the roughness under various feed rates is illustrated in Figure 7 (c). It is evident from the figure that better surface roughness distribution can be achieved with the feed rate of 2000 mm/min. It can be concluded that a satisfactory surface quality may be obtained when the optimum SPIF parameters are used.

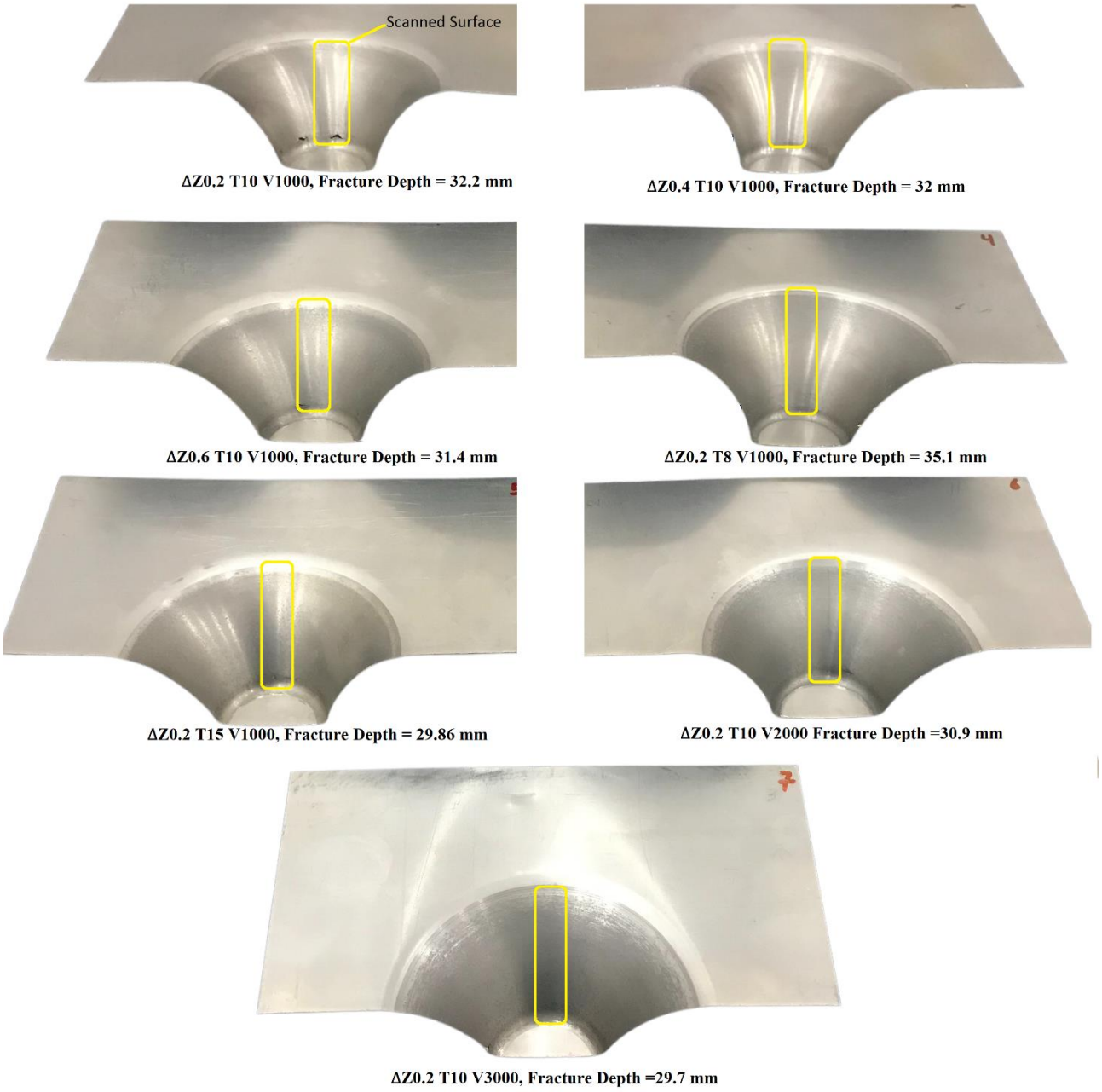

Figure 6 The scanned surface and fracture depth of hyperbolic truncated cones resulting from the SPIF under various process conditions (i.e., ΔZ=step size, T=tool diameter, and V=feed rate).

Figure 8 shows the inner surface of the truncated cone (scanned surface) from the top (right hand) to the bottom (left hand) of the cone. It is observed that there is a burnishing area, and step-down ridges start from the transition area between the top of the cone and the inclined wall and disappear gradually with increasing the depth of the cone. With a small step size (0.2 mm) and tool diameter (8 mm), and a low feed rate of 1000 mm/min, the ridges are clearer, and they are reduced when the step size, tool diameter, and feed rate are increased. The step-down ridges and burnishing are generated at the beginning of the SPIF process (low wall angle) because the truncated cone with a low wall angle is subjected to a low amount of stretching force. With increased amount of stretching force due to the long tool traveling (high wall angle) the step-down ridges and burnishing are disappeared.

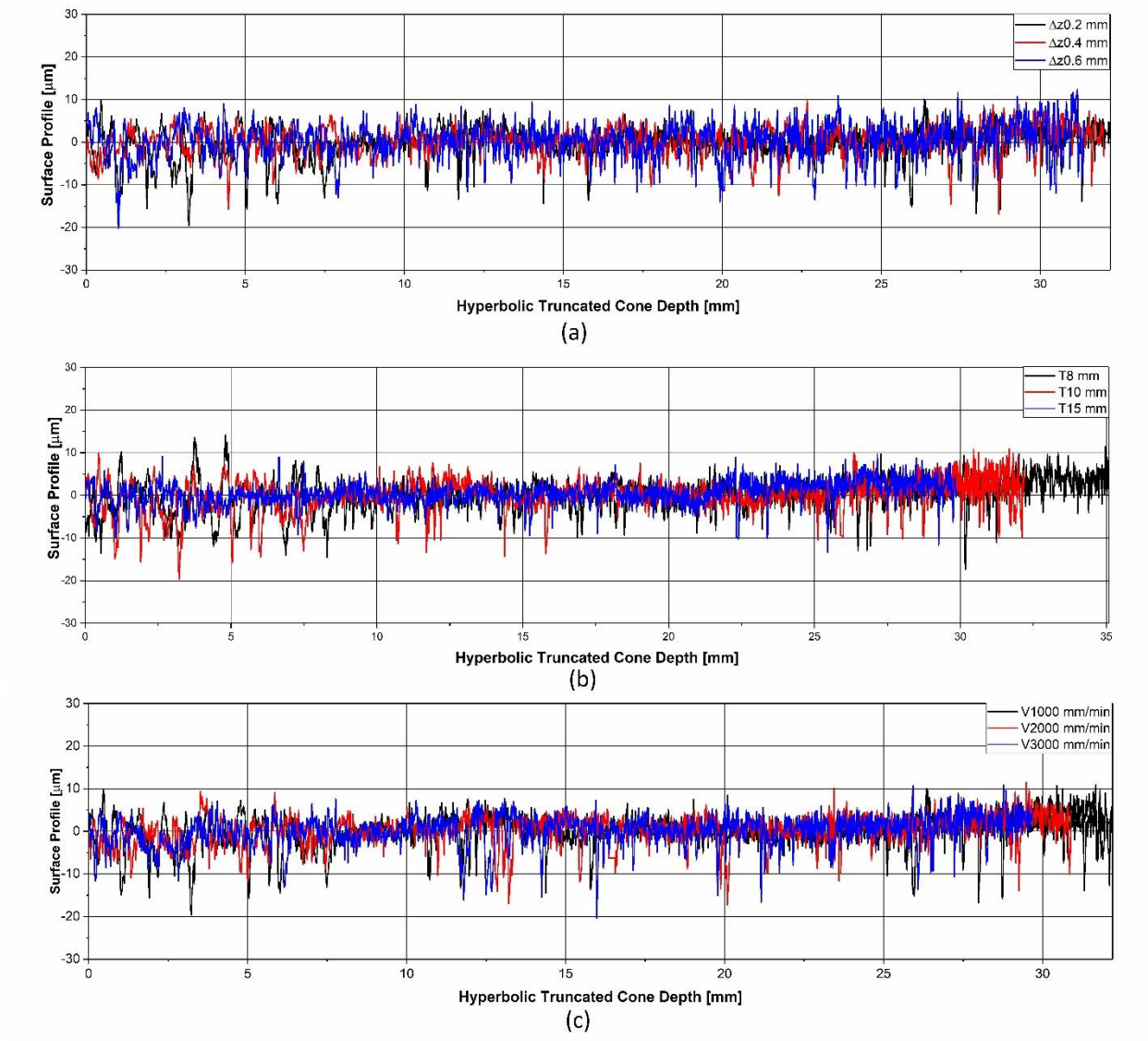

Figure 7 Effect of SPIF parameters surface roughness distribution along the hyperbolic truncated cone: (a) effect of step size, (b) effect tool diameter, and (c) effect of feed rate.

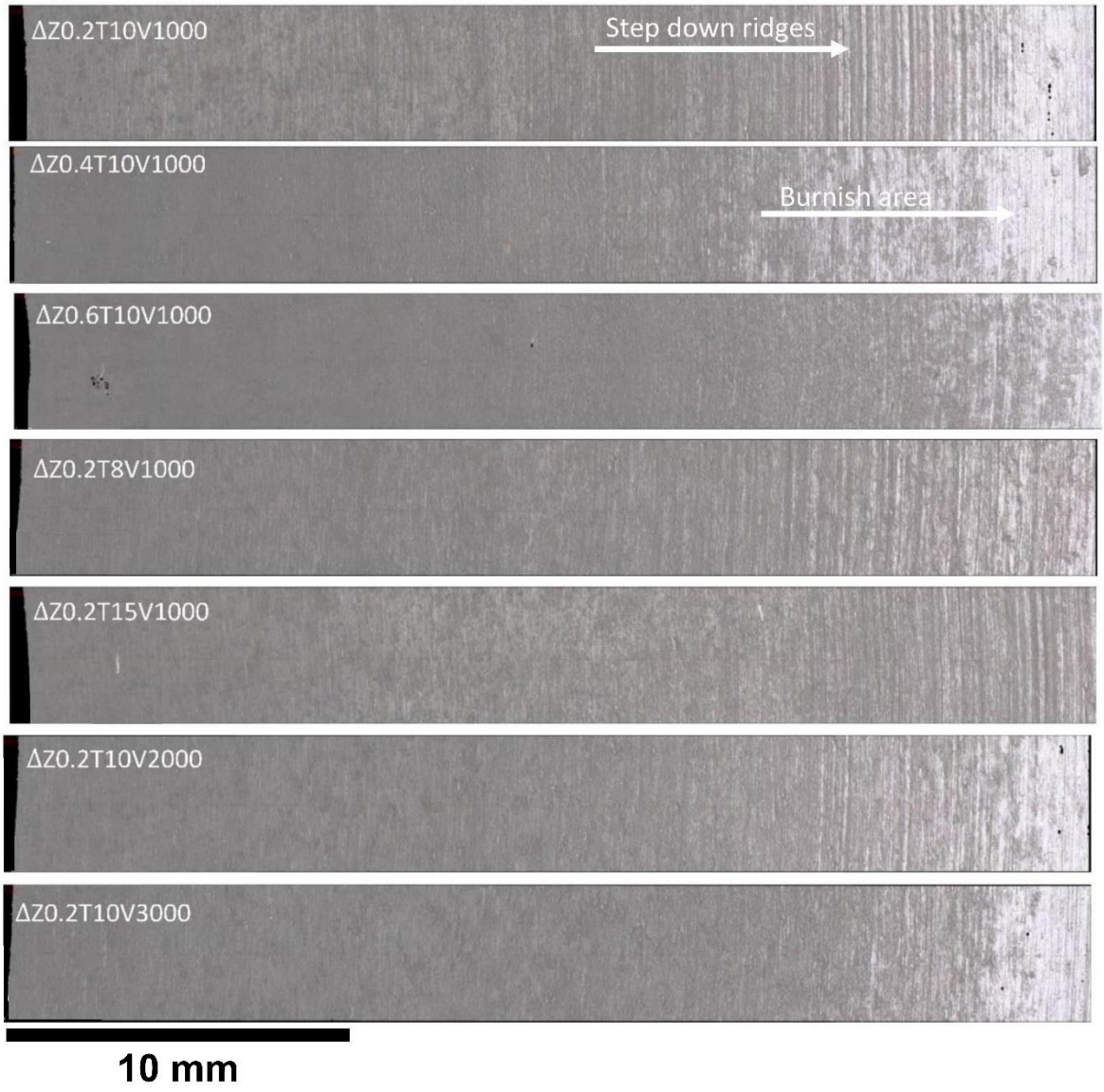

Figure 8 Topography of deformed pure titanium sheet under different SPIF parameters.

Abaqus/Explicit was used to simulate the SPIF process and to predict the equivalent stress and equivalent plastic strain along the wall of the truncated cone part from the top to the fractured region to determine the relationship between the stress, strain, and roughness distribution. The average value of stress from each element along the wall was drawn relative to the forming depth. Three step size values of 0.2, 0.4, and 0.6 mm with a constant tool diameter (10 mm) and feed rate (1000 mm/min) were used to investigate the effect of step size on the stress distribution. Figure 9 (a) demonstrates the distribution of the stress along the truncated cone wall under different step sizes. It is clear from the figure that high values of stress at the transition region between the top and inclined wall of the cone and this stress is reduced gradually until a certain value then becomes almost constant. High stress could be produced with the large value of step size and it is reduced

with small values of step size. The figure also shows that the high-stress values accelerate the fracture in the deformed truncated cone and this result in agreement with previous works by Hussain et al.[28] and Abd Ali et al. [29]. This is due to high level of stretching achieved with large step size and this leads to high stress values. In addition, with the large step size, the sheet is deformed by the action of the forming tool and by pulling, and this pull is reduced with a small step size. It is obvious from the figure that the components fail at different step sizes with the same degree of stress. The tool diameter was set to three values of 8, 10, and 15 mm with a constant step size (0.2 mm) and feed rate (1000 mm/min) to predict the impact of the tool diameter on the induced stress. The stress distribution varies with the size of the tool, the large diameter of the tool produces higher level of stress than that by a small diameter of the tool, as shown in Figure 9 (b). Furthermore, Figure 9(b) shows that low stress values increase the fracture depth of the truncated cone, and these findings are consistent with previous investigations [28-30]. This could be attributed to the interface region between the forming tool and the sheet. A large interface region with a large tool diameter leads to a high forming force and stress, and this is due to the localised deformation zone that could be produced with a small tool diameter, and this zone with a large tool diameter is decreased or becomes less localised. Similar to the effect of the step size, the formed parts by different tool sizes fail approximately at the same level of the stress.

Three values of feed rate 1000, 2000, and 3000 mm/min were utilised with a constant step size (0.2 mm) and tool diameter (10 mm) to demonstrate the influence of the feed rate on the stress distribution. Generally, the majority of materials produces high stress under high strain rate. In the SPIF process, the strain rate value is determined by the feed rate. A high strain rate is obtained with a high feed rate, which leads to high stress in the formed part as shown in Figure 9 (c). From the figure, the stress levels change from high at the beginning of forming (low wall angle) and reduce during the SPIF process to reach the lowest level at fracture. It is also clear from the figure that a high feed rate works to accelerate the fracture of the truncated cone, i.e., low fracture depth is produced at a high feed rate. This result is in agreement with previous works of Hussain et al. [28] and Ham and Jeswiet [31].

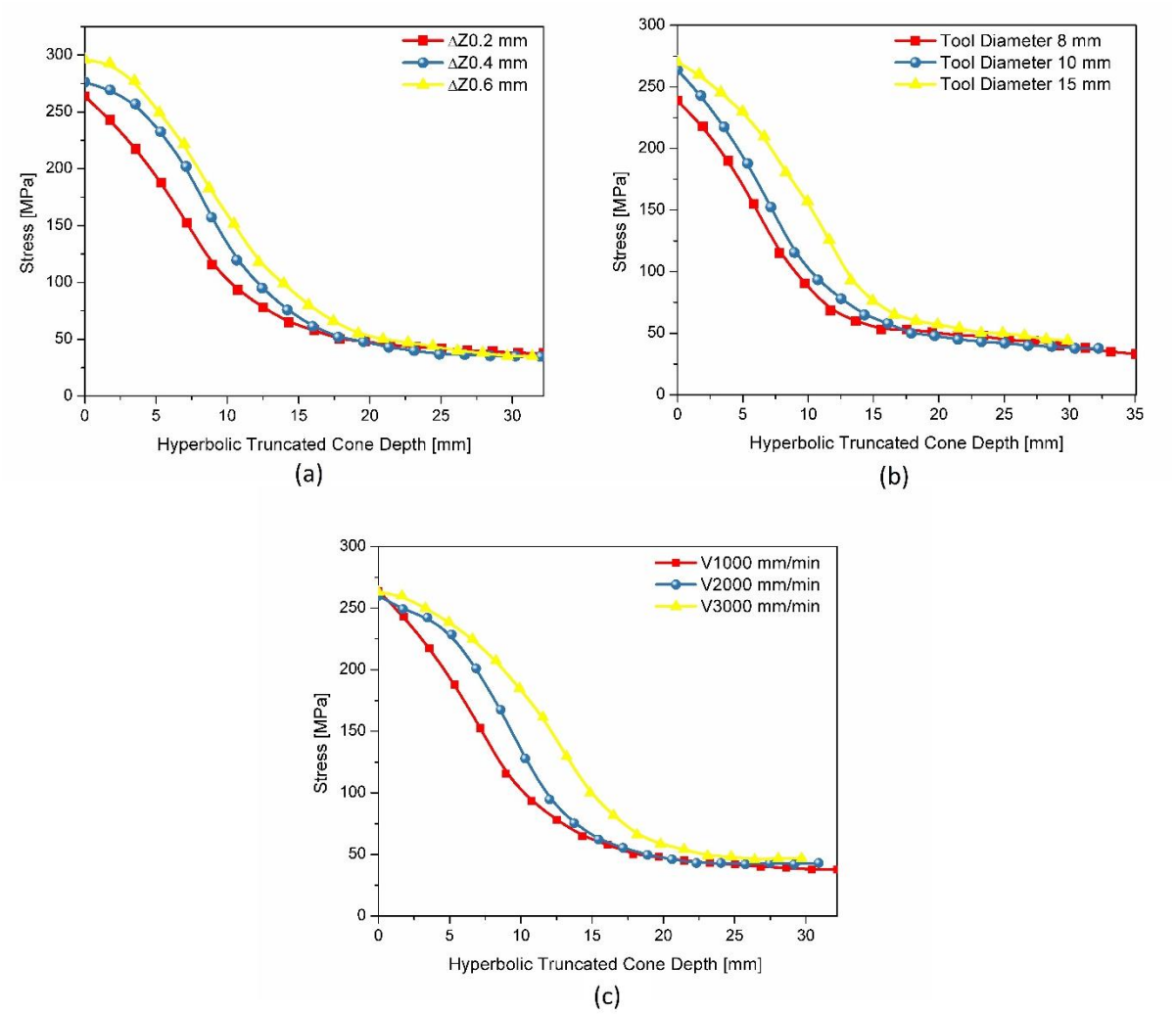

Figure 9 Mises stress distribution under different SPIF parameters: (a) effect of step size, (b) effect of tool diameter, and (c) effect of feed rate.

The effect of the SPIF parameters on the equivalent plastic strain was investigated under the same conditions as the distribution of stress. It was found that the profile of strain distribution starts from low values at the beginning of the SPIF process and increases progressively to reach the maximum value at the fracture as shown in Figure 10. It is obvious from the figure that the distribution of the strain is modified with the SPIF parameters and that high values of equivalent plastic strain could be due to large step size, tool diameter, and feed rate. It can be concluded that the large step size and tool diameter created a large amount of deformation, which results in an increase in the equivalent plastic strain. within the case of high feed rate, the temperature increase improves the capability of the material to deform and increase the strain values.

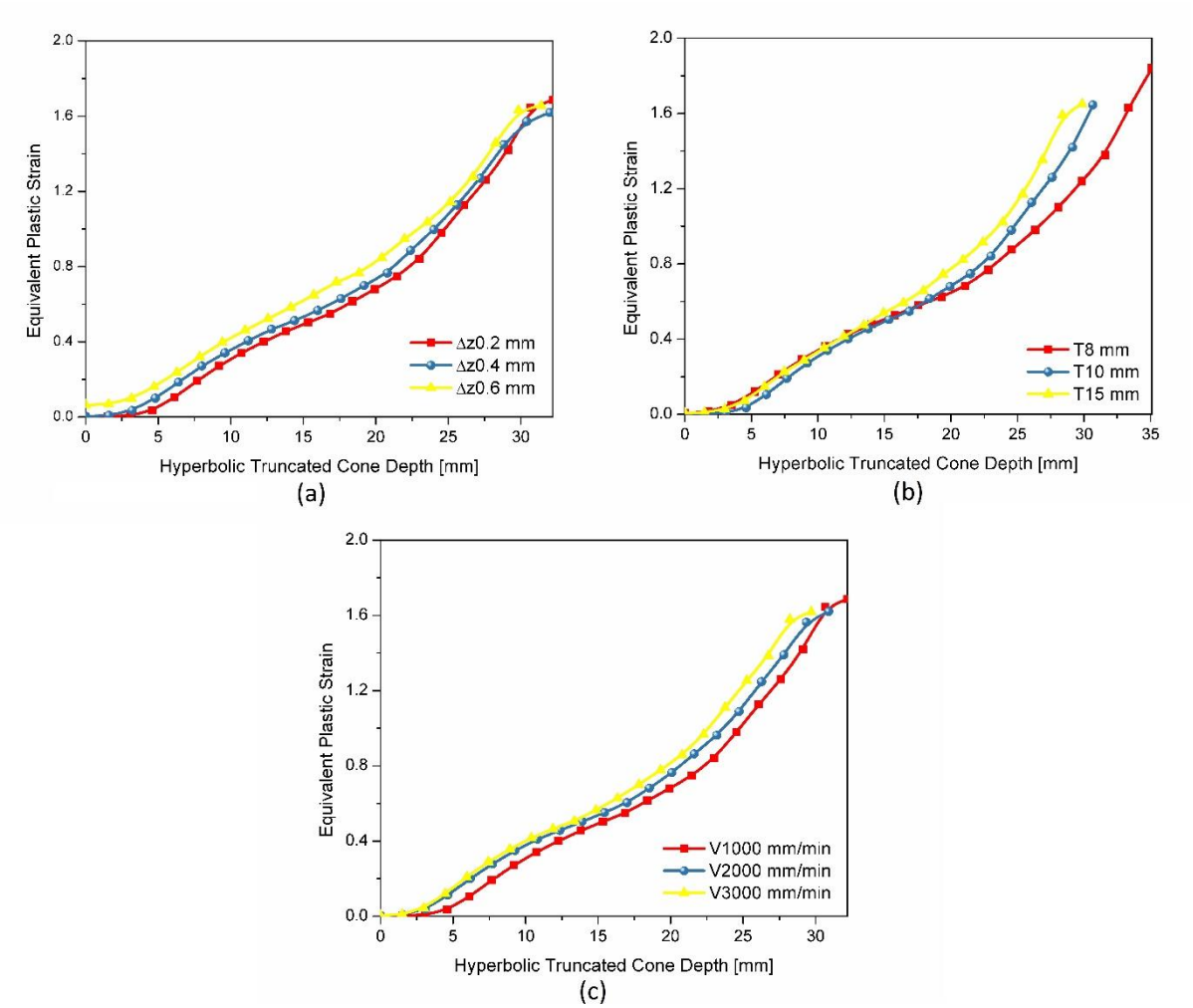

Figure 10 Equivalent plastic strain distribution under different SPIF parameters: (a) effect of step size, (b) effect of tool diameter, and (c) effect of feed rate.

From Figures 9 and 10, it can be concluded that under different SPIF conditions, the high stress-low strain region is produced at the beginning of the SPIF process (low wall angle) and, with an increase in the depth of the hyperbolic truncated cone (high wall angle), this region sustains a level of low stress and high strain as shown in Figure 11.

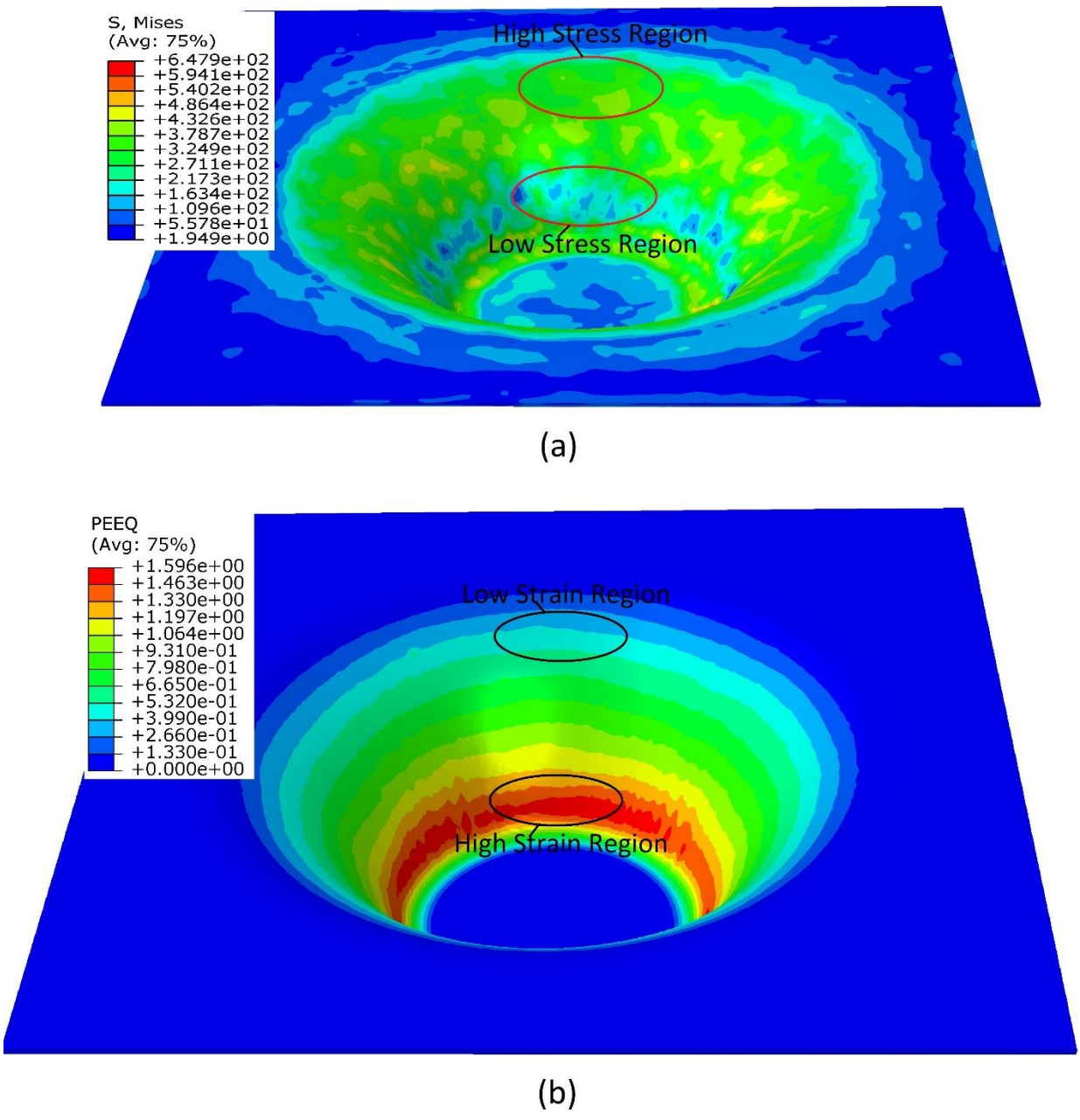

Figure 11 Distribution of the equivalent stress [MPa] (a) and equivalent plastic strain (b) obtained by numerical simulation of hyperbolic truncated cone.

Figure 12 depicts the relationship between the stress, equivalent plastic strain, and surface profile distribution under different step sizes and constant feed rate (1000 mm/min) and tool diameter (10 mm). It is observed from the figure that at the beginning of the SPIF process (low wall angle) with high values of stress and low strain values the height of waviness and the distance between the surface waviness are large and that is more evident with small step size (0.2 mm). Therefore, a rough surface is produced at the beginning of the SPIF process with a low forming angle (see Figure 8).

With increasing the forming depth, the peaks to valleys of the surface profile gradually become finer and the space between waves is reduced. Uniform distribution of the surface profile is observed with a large step size and the produced parts have a better surface quality. The effect of the tool diameter on the relationship between the surface profile roughness, stress, and plastic strain was investigated using three tool diameters, i.e., 8, 10, and 15 mm at a constant step size (0.2 mm) and feed rate (1000 mm/min) as shown in Figure 13. It can be seen that from the figure a large gap between the waviness and space between peaks and valleys is increased in the region of high stress and low plastic strain with 8 mm and 10 mm tool diameter. Better surface finish with uniform wave distribution could be achieved with a 15 mm tool diameter. Under all tool sizes, the profile of surface roughness becomes more uniform with increased depth of the truncated cone (high forming angle). Three feed rate values of 1000, 2000, and 3000 mm/ min at a constant step size (0.2 mm) and tool diameter (10 mm) were used to evaluate the effect of the feed rate on the surface quality of the deformed component. Under different feed rates, the relationship between the surface profile, stress, and the plastic strain is not consistent as shown in Figure 14. In the region of high- stress low strain (low wall angle) with feed rate 1000 mm/min the distance between the waviness is wide, and the height of waves is considered high as compared to the high wall angle region. With the feed rate at 2000 mm/min, the distribution of roughness is enhanced, and with 3000 mm/min the gap between the waviness gets larger again but is still less than 1000 mm/min. It is evident from the results that the best distribution of the surface profile could be achieved with a feed rate of 2000 mm/min under various feed rates. It is clear from Figures 12 to 14 that there is a relationship between the surface roughness profile and the formability of the materials as well as a uniform surface profile that could be produced with high formability. Furthermore, the surface roughness and equivalent stress and plastic strain correlation have a clear implication to the design and the surface quality of sheet parts made by the SPIF process.

It can be concluded from Figures 12 to 14 that a smooth surface is produced in the region of low stress-high strain (high forming angle), while a rougher surface is created in the region of high stress-low strain (low forming angle) as shown in Figure 15. This is due to the fact that the formed part is subjected to high stretching with an increase in the formed part depth. The overlap between the adjacent paths increases with increased forming angle, which led to the disappearance of the undeformed region between the adjacent paths. The same trend has been identified in previous studies of Yamashita et al. [32] and Cao and co-workers [7].

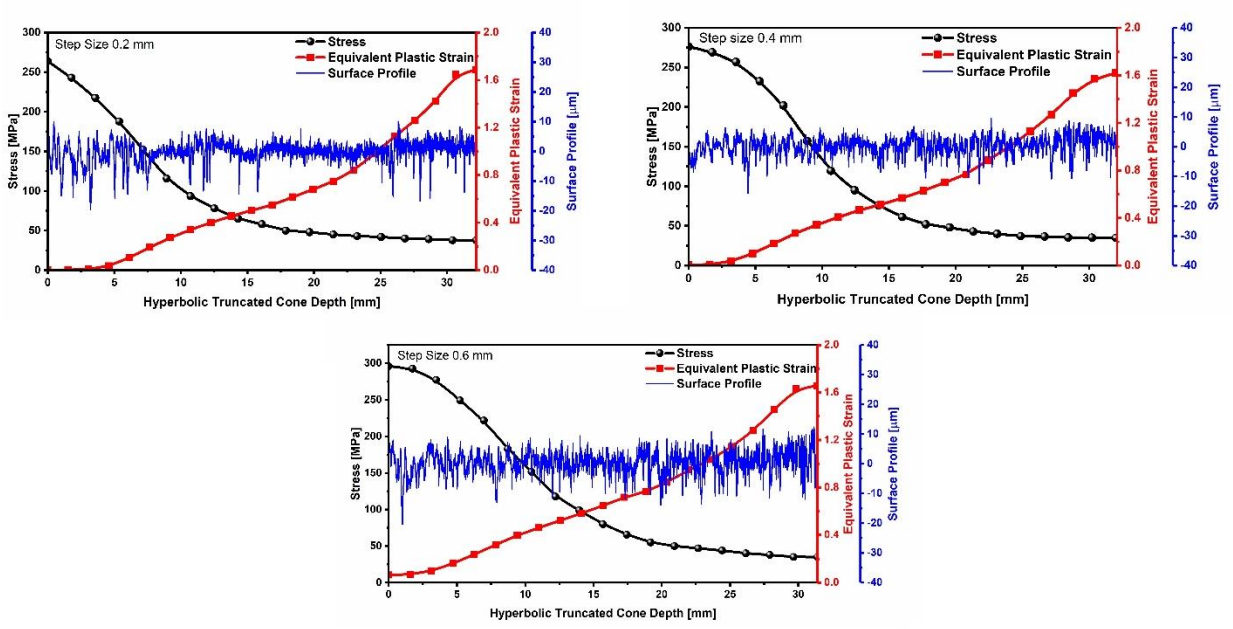

Figure 12 The relationship between the surface profile and stress and equivalent plastic strain with different step sizes.

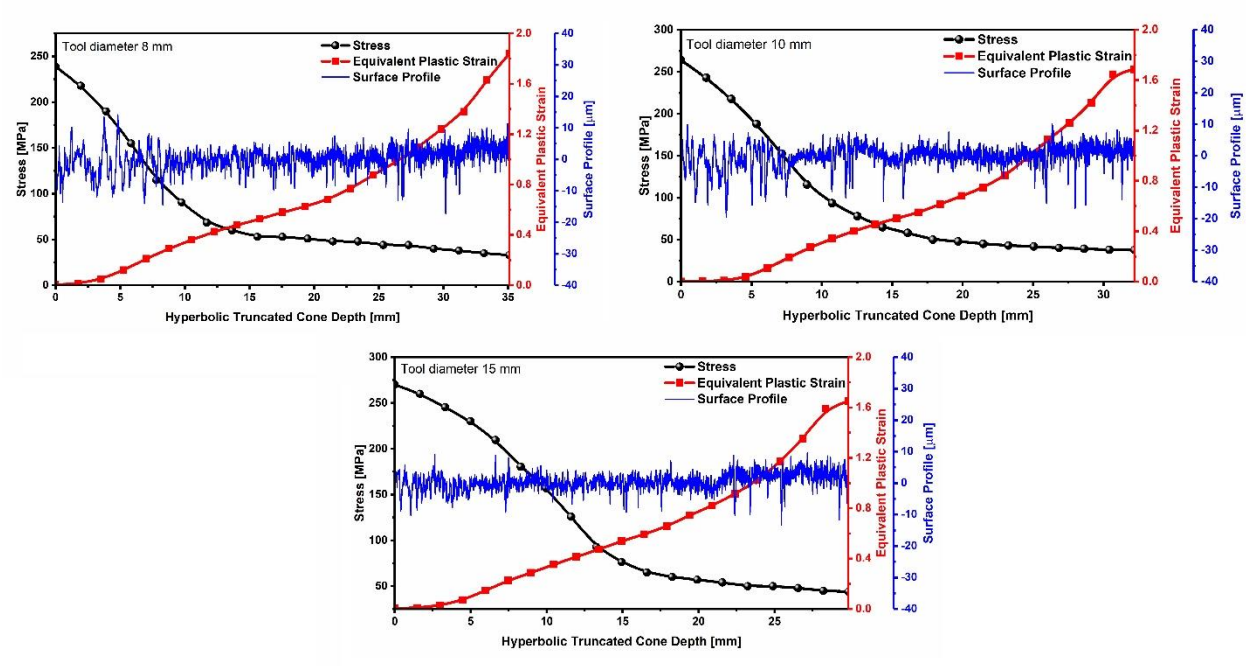

Figure 13 The relationship between the surface profile and stress and equivalent plastic strain with different tool diameters.

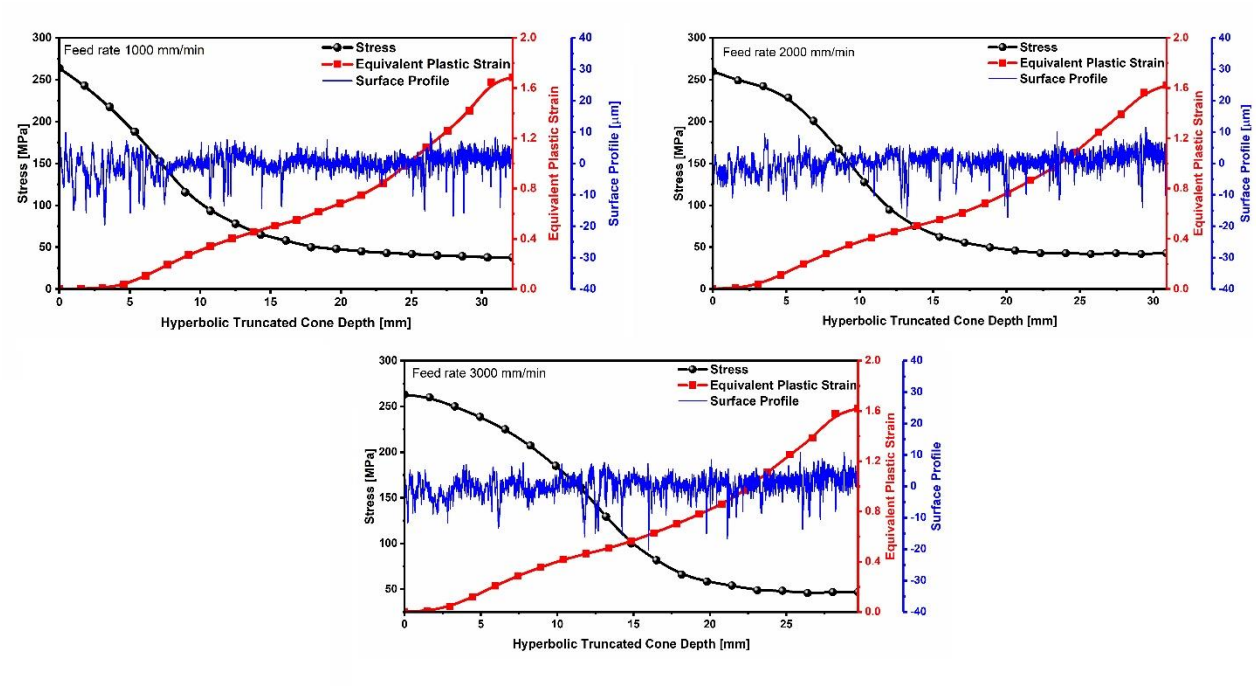

Figure 14 The relationship between the surface profile and stress and equivalent plastic strain with different feed rates.

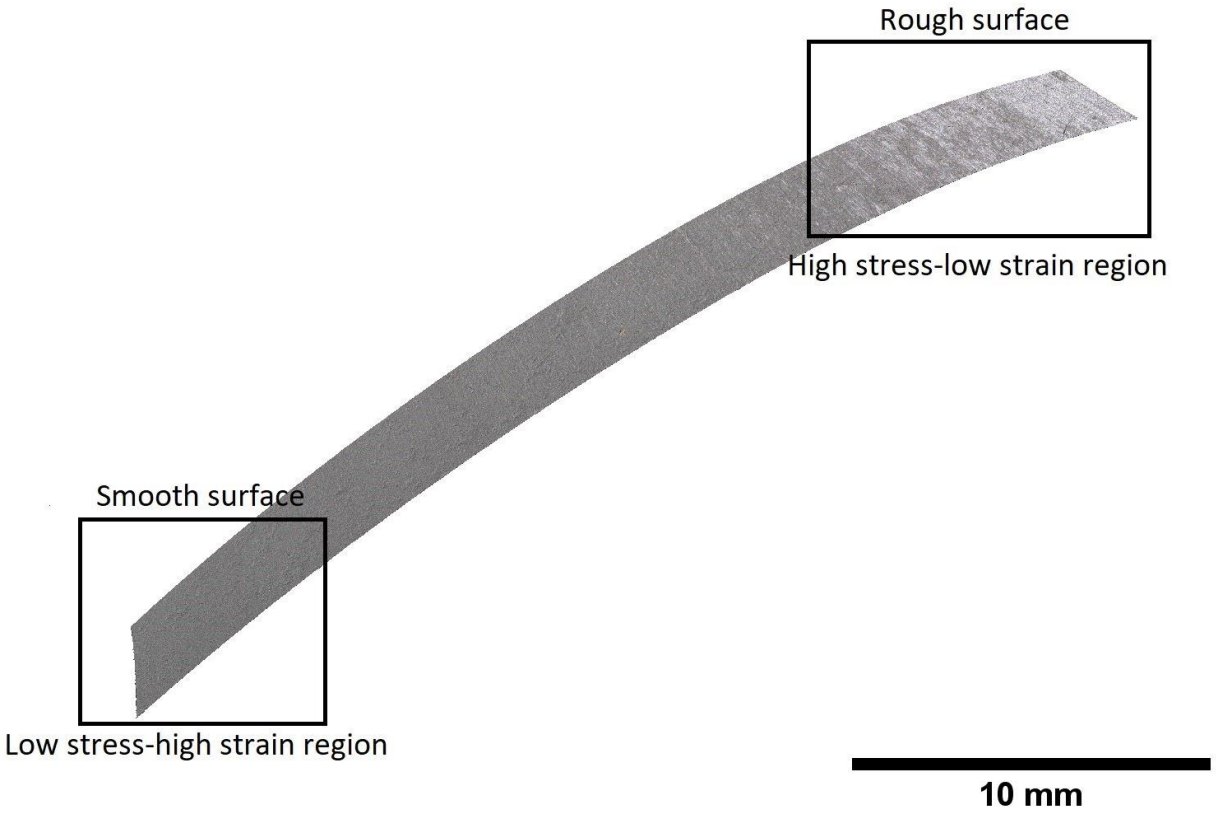

Figure 15 Surface roughness of hyperbolic truncated cone in high stress-low strain and low stress-high strain regions.

4. Conclusions

Based on experimental testing and FE simulation, this research investigated surface roughness of the pure titanium sheet formed by using the SPIF process under various forming conditions (i.e., tool diameter, step size, and feed rate). The roughness was measured along the wall of the hyperbolic truncated cone from the top to the fracture zone to determine the relation between the surface roughness profile and the stress and strain state. Alicona G4 Infinite Focus (IF) system was used to measure the surface roughness of the deformed pure titanium sheets. A 3D FE model of the SPIF process was developed using Abaqus/Explicit to predict the equivalent stress and the equivalent plastic strain distribution of the deformed components. The main conclusions of this work could be drawn as follows:

1. The surface roughness changes with the height of the deformed part. To gain a better understanding of the surface quality of the deformed SPIF components, consideration should be given to the overall surface along the product wall.
2. In the deformed SPIF components, a burnishing region and step-down ridges starts from the transition area between the top of the cone and the inclined wall and gradually disappears with an increase in the depth of the hyperbolic truncated cone. The height of the surface waviness, and the gap between the surface waviness is high in this region and this is more apparent with a low level of the SPIF parameters. The height of surface waviness and the distance between the surface waviness could change when the SPIF parameters are altered.
3. Rough surface could be produced in the region of high stress low equivalent plastic strain (low wall angle). High-stress values are generated in the transition region between the top and the inclined wall of the cone, and this stress is gradually decreased until a certain almost constant value Moreover, the SPIF components fail at the same stress level under different SPIF conditions.
4. The experimental and FE results revealed that there is a correlation between the stress-strain conditions, the forming stage of the SPIF process, the SPIF parameters, and the surface roughness, which may be helpful in the design and ISF operation of the component where a higher-level criterion for the surface finish is an essential factor.
5. The overall surface roughness of the pure Ti sheets was assessed under a plane strain condition (hyperbolic truncated cone) using three forming parameters, e.g., tool diameter, step size and feed rate. Further research will be conducted to investigate the surface quality

of different shapes (different strain states), i.e., a straight-sided cone, hyperbolic truncated pyramid, and a dome shape, in order to establish a relationship between surface roughness and strain state. In addition, the effect of other parameters of the SPIF process, such as tool rotation, tool shape and type of materials, on the overall surface roughness will also need to be investigated.

Acknowledgements

The authors wish to thank Prof. Jun Chen of the Department of Plasticity Technology, Shanghai Jiao Tong University, China for his support to perform the SPIF testing, Dr. Tahseen Jwad of the School of the Mechanical Engineering University of Birmingham, the UK for his support in surface roughness measurements.

References

1. Gatea, S., H. Ou, and G. McCartney, *Review on the influence of process parameters in incremental sheet forming.* The International Journal of Advanced Manufacturing Technology, 2016. **87**(1-4): p. 479-499.
2. Cerro, I., E. Maidagan, J. Arana, A. Rivero, and P. Rodriguez, *Theoretical and experimental analysis of the dieless incremental sheet forming process.* Journal of Materials Processing Technology, 2006. **177**(1-3): p. 404-408.
3. Attanasio, A., E. Ceretti, C. Giardini, and L. Mazzoni, *Asymmetric two points incremental forming: improving surface quality and geometric accuracy by tool path optimization.* Journal of materials processing technology, 2008. **197**(1-3): p. 59-67.
4. Durante, M., A. Formisano, A. Langella, and F.M.C. Minutolo, *The influence of tool rotation on an incremental forming process.* Journal of Materials Processing Technology, 2009. **209**(9): p. 4621-4626.
5. Hamilton, K. and J. Jeswiet, *Single point incremental forming at high feed rates and rotational speeds: Surface and structural consequences.* CIRP annals, 2010. **59**(1): p. 311-314.
6. Oleksik, V., A. Pascu, C. Deac, R. Fleacă, O. Bologa, and G. Racz, *Experimental study on the surface quality of the medical implants obtained by single point incremental forming.* International Journal of Material Forming, 2010. **3**(1): p. 935-938.
7. Bhattacharya, A., K. Maneesh, N. Venkata Reddy, and J. Cao, *Formability and surface finish studies in single point incremental forming.* Journal of manufacturing science and engineering, 2011. **133**(6).
8. Ambrogio, G., L. Filice, and F. Gagliardi, *Formability of lightweight alloys by hot incremental sheet forming.* Materials & Design, 2012. **34**: p. 501-508.
9. Lu, B., J. Chen, H. Ou, and J. Cao, *Feature-based tool path generation approach for incremental sheet forming process.* Journal of Materials Processing Technology, 2013. **213**(7): p. 1221-1233.
10. Ham, M., B. Powers, and J. Loiselle. *Surface topography from single point incremental forming using an acetal tool*. in *Key Engineering Materials*. 2013. Trans Tech Publ.
11. Mugendiran, V., A. Gnanavelbabu, and R. Ramadoss, *Parameter optimization for surface roughness and wall thickness on AA5052 Aluminium alloy by incremental forming using response surface methodology.* Procedia Engineering, 2014. **97**: p. 1991-2000.
12. Lu, B., Y. Fang, D. Xu, J. Chen, H. Ou, N. Moser, and J. Cao, *Mechanism investigation of friction-related effects in single point incremental forming using a developed oblique roller-ball tool.* International Journal of Machine Tools and Manufacture, 2014. **85**: p. 14-29.

13. Kurra, S., N.H. Rahman, S.P. Regalla, and A.K. Gupta, *Modeling and optimization of surface roughness in single point incremental forming process.* Journal of Materials Research and Technology, 2015. **4**(3): p. 304-313.
14. Gatea, S., D. Xu, H. Ou, and G. McCartney, *Evaluation of formability and fracture of pure titanium in incremental sheet forming.* The International Journal of Advanced Manufacturing Technology, 2018. **95**(1-4): p. 625-641.
15. Mulay, A., B.S. Ben, S. Ismail, and A. Kocanda, *Prediction of average surface roughness and formability in single point incremental forming using artificial neural network.* Archives of Civil and Mechanical Engineering, 2019. **19**: p. 1135-1149.
16. Sakhtemanian, M., M. Honarpisheh, and S. Amini, *A novel material modeling technique in the single-point incremental forming assisted by the ultrasonic vibration of low carbon steel/commercially pure titanium bimetal sheet.* The International Journal of Advanced Manufacturing Technology, 2019. **102**(1-4): p. 473-486.
17. Gupta, P., A. Szekeres, and J. Jeswiet, *Design and development of an aerospace component with single-point incremental forming.* The International Journal of Advanced Manufacturing Technology, 2019. **103**(9-12): p. 3683-3702.
18. Tera, M., R.-E. Breaz, S.-G. Racz, and C.-E. Girjob, *Processing strategies for single point incremental forming—a CAM approach.* The International Journal of Advanced Manufacturing Technology, 2019. **102**(5-8): p. 1761-1777.
19. Durante, M., A. Formisano, and F. Lambiase, *Formability of polycarbonate sheets in single-point incremental forming.* The International Journal of Advanced Manufacturing Technology, 2019. **102**(5-8): p. 2049-2062.
20. Dakhli, M., A. Boulila, P.-Y. Manach, and Z. Tourki, *Optimization of processing parameters and surface roughness of metallic sheets plastically deformed by incremental forming process.* The International Journal of Advanced Manufacturing Technology, 2019. **102**(1-4): p. 977-990.
21. Vahdani, M., M.J. Mirnia, H. Gorji, and M. Bakhshi-Jooybari, *Experimental Investigation of Formability and Surface Finish into Resistance Single-Point Incremental Forming of Ti–6Al–4V Titanium Alloy Using Taguchi Design.* Transactions of the Indian Institute of Metals, 2019. **72**(4): p. 1031-1041.
22. Ramkumar, K., N. Baskar, K. Elangovan, C.S. Narayanan, K. Selvarajan, and C. Jesuthanam, *Comparison of Multi Point Incremental Forming Tool with Single Point Incremental Forming Tool Using FLD, Fractography and 3D-Surface Roughness Analysis on Cr/Mn/Ni/Si Based Stainless Steel.* Silicon, 2020: p. 1-8.
23. Chang, Z. and J. Chen, *Analytical model and experimental validation of surface roughness for incremental sheet metal forming parts.* International Journal of Machine Tools and Manufacture, 2019. **146**: p. 103453.
24. He, A., M.P. Kearney, K.J. Weegink, C. Wang, S. Liu, and P.A. Meehan, *A model predictive path control algorithm of single-point incremental forming for non-convex shapes.* The International Journal of Advanced Manufacturing Technology, 2020. **107**(1): p. 123-143.
25. Kulkarni, S.S. and G.M. Mocko, *Experimental investigation and finite element modeling of localized heating in convective heat-assisted single-point incremental forming.* The International Journal of Advanced Manufacturing Technology, 2020. **107**(1): p. 945-957.
26. Vahdati, M., M. Sedighi, and H. Khoshkish. *An analytical model to reduce spring-back in incremental sheet metal forming (ISMF) process*. in *Advanced Materials Research*. 2010. Trans Tech Publ.
27. Silva, P.J., L.M. Leodido, and C.R.M. Silva. *Analysis of incremental sheet forming parameters and tools aimed at rapid prototyping*. in *Key Engineering Materials*. 2013. Trans Tech Publ.
28. Hussain, G., L. Gao, and Z. Zhang, *Formability evaluation of a pure titanium sheet in the cold incremental forming process.* The International Journal of Advanced Manufacturing Technology, 2008. **37**(9-10): p. 920-926.
29. Abd Ali, R., W. Chen, K. Jin, Y. Bao, and A.W. Hussein, *Formability and failure analyses of Al/SUS bilayer sheet in single point incremental forming.* The International Journal of Advanced Manufacturing Technology, 2019. **105**(7-8): p. 2785-2798.

30. Silva, M.B., P.S. Nielsen, N. Bay, and P. Martins, *Failure mechanisms in single-point incremental forming of metals.* The International Journal of Advanced Manufacturing Technology, 2011. **56**(9-12): p. 893-903.
31. Ham, M. and J. Jeswiet, *Single point incremental forming and the forming criteria for AA3003.* CIRP annals, 2006. **55**(1): p. 241-244.
32. Yamashita, M., M. Gotoh, and S.-Y. Atsumi, *Numerical simulation of incremental forming of sheet metal.* Journal of materials processing technology, 2008. **199**(1-3): p. 163-172.

Declarations

Paper title: Surface roughness analysis of medical grade titanium sheets formed by single point incremental forming

Authors: Shakir Gatea and Hengan Ou

Funding (Not applicable)

Conflicts of interest/Competing interests (Not applicable)

Availability of data and material (Data and materials are available)

Code availability (Not applicable)

Authors' contributions (Shakir Gatea designed the study, performed experiments, and wrote the manuscript; **Hengan Ou** designed the study and contributed to the data interpretation)

Ethics approval (Not applicable)

Consent to participate (I am agreeing to participate)

Consent for publication (I am agreeing to publish this work)

Shakir Gatea